Swept-3-D Ultrasound Imaging of the Mouse Brain Using a Continuously Moving 1-D-Array—Part I: Doppler Imaging

Bastian S. Generowicz, Stephanie Dijkhuizen, Chris I. De Zeeuw, Sebastiaan K. E. Koekkoek, and Pieter Kruizinga

***Abstract*—Volumetric 3-D Doppler ultrasound imaging can be used to investigate large scale blood dynamics outside of the limited view that conventional 2-D power Doppler images (PDIs) provide. To create 3-D PDIs, 2-D-matrix array transducers can be used to insonify a large volume for every transmission; however, these matrices suffer from low sensitivity, high complexity, and high cost. More typically, a 1-D-array transducer is used to scan a series of stationary 2-D PDIs, after which a 3-D volume is created by concatenating the 2-D PDIs in post-processing, which results in long scan times due to repeated measurements. Our objective was to achieve volumetric 3-D Doppler ultrasound imaging with a high Doppler sensitivity, similar to that of a typical stationary recording using a 1-D-array transducer, while being more affordable than using 2-D-matrix arrays. We achieved this by mounting a 1-D-array transducer to a high-precision motorized linear stage and continuously translating over the mouse brain in a sweeping manner. For Part I of this article, we focused on creating the best vascular images by investigating how to best combine filtered beamformed ultrasound frames, which were not acquired at the same spatial locations, into PDIs. Part II focuses on the implications of sampling transient brain hemodynamics through functional ultrasound (fUS) while continuously translating over the mouse brain. In Part I, we show how the speed at which we sweep our 1-D-array transducer affects the Doppler spectrum in a flow phantom. In vivo recordings were performed on the mouse brain while varying the sweeping speed, showing how higher sweeping speeds negatively affect the PDI quality. A weighting vector is found to combine frames while continuously moving over the mouse brain, allowing us to create swept PDIs of similar sensitivity when compared with those obtained using a stationary 1-D-array while allowing a significantly higher 3-D Doppler volume rate and maintaining the benefits of having a low computational and monetary cost. We show that a vascular subvolume of 6 mm can be scanned in 2.5 s, with a PDI reconstructed every 200 μm, outperforming classical staged recording methods.**

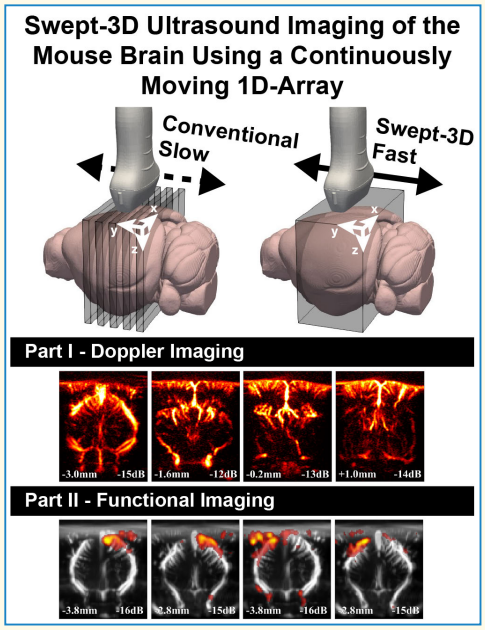

***Index Terms*—3-D Doppler imaging, 3-D mouse brain, Doppler flow phantom, motorized linear stage, volumetric Doppler imaging.**

Manuscript received 28 July 2023; accepted 19 September 2023. Date of publication 3 October 2023; date of current version 13 December 2023. This publication is part of the project CUBE (with project number 108845) of the research programme NWO-groot which is partly financed by the Dutch Research Council (NWO). Financial support was also provided by The Erasmus MC (M-RACE 109969; PK), Erasmus University (Fellowship 109316; PK), NWO (NWO-ALW 824.02.001; CIDZ), the Dutch Organization for Medical Sciences (ZonMW 91120067; CIDZ), Medical Neuro-Delta (MD 01092019-31082023; CIDZ), INTENSE LSH-NWO (TTW/00798883; CIDZ), ERC-adv (GA-294775 CIDZ) van Raamsdonk fonds (NIN), as well as the NWO-Gravitation Program (DBI2). *(Corresponding author: Pieter Kruizinga.)*

This work involved human subjects or animals in its research. Approval of all ethical and experimental procedures and protocols was granted by the Institutional Animal Care and Use (IACUC) (Dutch Ethical Committee, Erasmus MC) under Project No. AVD1010020197846.

Please see the Acknowledgment section of this article for the author affiliations.

Digital Object Identifier 10.1109/TUFFC.2023.3318653

I. Introduction

HIGH frame rate power Doppler imaging is becoming a well-established tool in the field of neuroscience, where it is used to provide information on hemodynamics with high spatial and temporal resolutions. This technique makes use of high frame rate plane-wave ultrasound transmissions, which insonify the entire field of view in a single shot to create high frame rate power Doppler images (PDIs) [1], [2]. In the context of brain imaging, the magnitude of the PD signal is proportional to the cerebral blood volume (CBV) and therefore can be used to perform functional ultrasound (fUS) as, due to the mechanism of neurovascular coupling, the PD signal can be interpreted as a proxy for neuronal activity [3].

Highlights

- **We created swept-3-D PDIs by continuously translating a high-frequency 1-D-array transducer over a mouse brain using a high-precision motorized linear stage.**
- **Using our swept-3-D method, we show that a 6-mm subvolume of mouse brain vasculature can be scanned in 2.5 s, with a PDI of high sensitivity reconstructed every 200 μm.**
- **Our swept-3-D method can significantly reduce the required acquisition time of volumetric Doppler imaging when compared with the conventional staged acquisition techniques.**

Typically, PD ultrasound of the rodent brain, in our case the mouse brain, makes use of a high-frequency 1-D-array transducer to image a specific cross section of the brain. Logically, this resulting 2-D image of a cross section or brain slice is unable to provide blood flow characteristics outside of the insonified region and is therefore insufficient when measuring a complex 3-D system such as the brain.

Attempts have been made to use 2-D-matrix transducer arrays for 3-D Doppler ultrasound, which are able to insonify a 3-D volume at once using a single transmission [4], [5], [6]; however, these systems suffer from low sensitivity, high computational complexity, and high cost (both for the transducer and the hardware required to use it) when compared with the traditional 1-D-arrays. These dense 2-D arrays can also be undersampled using, for example, row–column addressing [7], which reduces the computational complexity of fully populated 2-D-arrays while not suffering from the poor elevation resolution of 1-D-array transducers and been successfully demonstrated on functional Doppler imaging of the rat brain [6], or through the use of sparse arrays [8] or μ-beamformers [9].

Methods for 3-D imaging using a 1-D-array most often require motorized stages to translate across the region of interest. Using this method, a stationary acquisition is repeated for every location resulting in long acquisition times [10], [11], [12], [13]. Alternatively, 3-D Doppler volumes can be reconstructed from nonstationary acquisitions if the location of each acquisition is known, such as by recording the position and orientation of the transducer in parallel to ultrasound recording [14], [15], which is particularly important in some clinical settings where free-hand recordings are necessary. A motorized linear translation stage can also be used to continuously translate a ultrasound transducer with a constant speed over a region of interest to create 3-D Doppler images, such as those shown of the kidney and breast lesions [16]. A mechanically swept transducer, or "Wobbler," can be used to create 3-D ultrasound scans by continuously translating over a known trajectory, converting its 2-D scans into a 3-D volume [17]. A Wobbler has an additional advantage of being enclosed in a casing, making it safe for use in more dynamic environments where the imaging region has inherent movement. In addition to a Wobbler, high volume rate 3-D ultrasound was also shown using fast tilting reflectors to steer the plane-wave acquisitions [18].

In practice, 3-D PDI volumes of the mouse brain are often used to register the ultrasound vascular imaging domain to the neuroanatomy commonly used in neuroscience, such as the Allen Brain Atlas [19] or Paxinos and Watson [20]. This allows the user to more reliably choose a specific imaging plane for further neuroscience measurements, which is a common problem when using a 2-D imaging modality in a complex 3-D structure. This registration recording typically consists of short recordings (e.g., 5 s) obtained at small spatial intervals (e.g., 100 μm) between the start and end of a craniotomy of a mouse brain (approx. 6 mm), resulting in a total recording duration of at least 5 min to create a 3-D volume, not taking into account safety margins and delays between successive slices. If multiple recordings are preformed over multiple sessions, the registration scan has to be repeated every time the mouse is placed into the setup, as inter-scanmotion makes it impractical to rely on previously obtained registration data.

We set out to achieve affordable and fast 3-D Doppler ultrasound of the mouse brain with a high signal-to-noise ratio (SNR). This was achieved by attaching a high-frequency 1-D-array ultrasound transducer to a high-precision programmable linear stage which is continuously moving over the mouse brain in a sweeping manner while continuously acquiring high frame rate Doppler ultrasound data. The *swept-3-D* method, as it will be called in this article, allows us to reconstruct a full 3-D PDI volume every time the transducer has moved from one limit to the next. For Part I of this two-part article, we will present methods for creating the best vascular images while continuously translating over the brain (seen as those that most closely resemble the PDIs acquired during a stationary staged acquisition), while also maintaining the integrity of the Doppler content of our signal. Part II is focused on using this swept-3-D technique to obtain 3-D functional images of the mouse brain aiming for high functional imaging sensitivity, fixating on the tradeoff between temporal resolution (and thus functional response) and PDI sensitivity. These two objectives are different as functional imaging poses constraints on the temporal sampling of every location due to the hemodynamic response to a stimulus in the Doppler signal, which limits the minimum sweeping speed of the 1-D-array transducer. This means that optimizing for the best vascular images poses a different problem to that when optimizing for functional sensitivity when it comes to sweeping speeds and averaging.

II. Swept-3-D Doppler Acquisition

A. Doppler Ultrasound Data Acquisition

The application of high frame rate Doppler ultrasound imaging on the rodent brain poses many unique criteria when considering a continuously moving acquisition such as

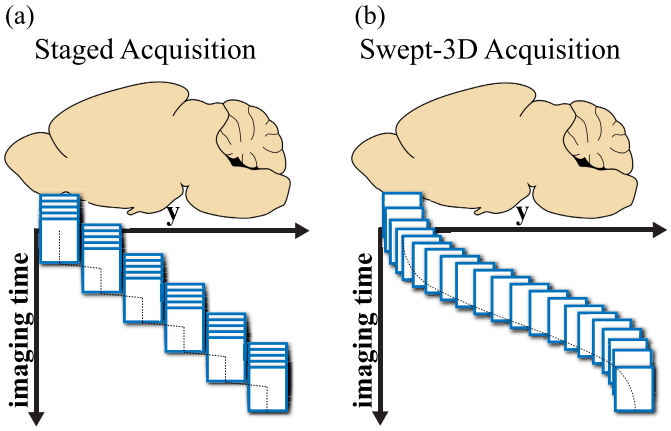

Fig. 1. Acquisition schemes for 3-D Doppler ultrasound of the mouse brain, comparing the conventional (a) *staged* acquisitions to the continuous acquisitions of our (b) *swept-3-D* acquisition method.

a relatively small scanning region, highly detailed vasculature requiring high-frequency 1-D-array transducer array, and a unique method of acquiring images. Each of these has an effect on the design choices and will be discussed in Sections II-A1–II-A6.

Most often, for 3-D Doppler ultrasound data acquisition of the mouse brain, a high-frequency 1-D-array transducer is attached to a motorized linear stage and repeated stationary recordings are performed, where the motorized stage moves the imaging plane to the next location between successive recordings, as shown in Fig. 1(a). PDIs from this so-called "staged" acquisition can then be concatenated to create a 3-D volume of the brain vasculature.

For the method proposed in this article, instead of only acquiring data while the ultrasound transducer is stationary, we continuously acquire high frame rate ultrasound data while scanning over the mouse brain in a swept manner, as highlighted in Fig. 1(b), where one translation from the start till the end of the craniotomy is named a "sweep."

1) System Hardware: To achieve reliable swept acquisitions, a high-precision motorized linear stage (X-LDA025A, Zaber Technologies Inc., Vancouver, BC, Canada) was required. During experimentation, it was observed that when the transducer was set to sweep at high speeds ($<\pm 3$ s per sweep over ± 6 mm distance), the motor was no longer able to accurately slow down the stage at the desired limit. It was therefore decided to minimize the load attached to the motorized stage by removing the casing of the ultrasound transducer, and replacing it with a custom, robust, and lightweight probe holder using a 3-D printer. The probe and custom mount were attached to the motorized stage as seen in Fig. 2. For ultrasound data acquisition of the mouse brain, a high-frequency 128-element linear transducer (L22-14v with a 0.1-mm pitch, 1.5-mm elevation, and 8-mm elevation focus) was coupled to a Verasonics acquisition system (Vantage 256 High Frequency), and was driven with a three-cycle burst of 18 MHz.

2) Acquisition Triggering: As the goal of this article was to create accurate 3-D Doppler reconstructions, the ultrasound acquisitions were linked to the displacement of the motorized stage. Every time the motorized stage had moved a specified distance, a trigger signal was sent to the Verasonics acquisition

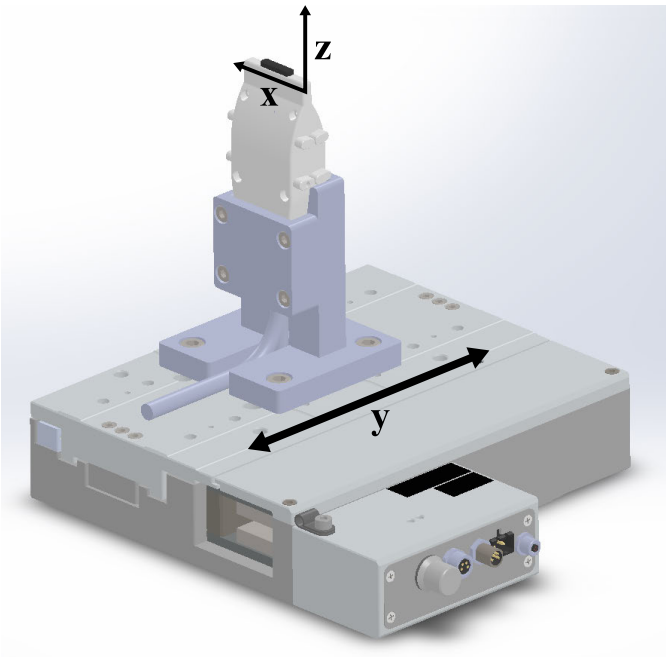

Fig. 2. Schematic of the L22-14v ultrasound transducer attached to a motorized linear stage using a custom probe holder. The *y*-axis shows the direction of movement of the linear stage, while the *x*- and *z*-axis show the imaging plane of the ultrasound transducer.

system, which initiated a plane-wave imaging sequence. With this method, the exact location of every acquired beamformed frame is known, which is helpful for 3-D reconstructions and when comparing the swept recordings to those obtained using a stationary recording. This method has a benefit that it becomes easier to accurately combine frames acquired at the same location during multiple sweeps if desired, such as is the case for functional recordings which will be investigated further in Part II of this article.

Typically, for the generation of real-time high frame rate PDIs, a fixed pulse repetition frequency (PRF) is taken. For swept-3-D acquisitions, as the speed at which the motorized stage is moving is not constant throughout the sweep, our PRF is linked to the speed of the motorized stage, which varies over its trajectory. Therefore, we decided to decouple the transmission PRF (time between angled plane waves) from the Doppler FR (time between a set of angled plane waves, which is not to be confused with the PDI frame rate, where an ensemble of Doppler frames are averaged to create a PDI).

For every trigger the Verasonics receives from the motorized stage, a series of eight angled plane waves (N_a) between $\pm 9°$ were recorded and compounded into a single beamformed frame in real-time, all while the motorized stage is continuously moving as highlighted in Fig. 3. After beamforming, the ultrasound system waits for its next trigger from the motorized stage, which occurs once it has moved a specified distance. These high frame rate beamformed data were then stored on a fast SSD for postprocessing. Due to the continuous motion during acquisitions, N_a is ideally kept as low as possible, since the raw frames are not recorded at exactly the same location. The number of angles was chosen based on the diminishing returns in contrast for higher N_a shown by Bercoff et al. [21], where this number was found to strike a good balance between SNR and acquisition length.

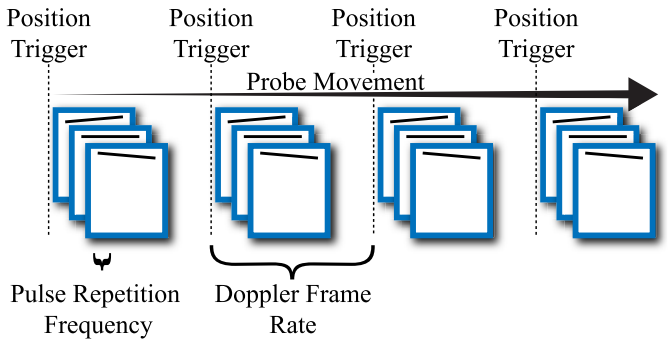

Fig. 3. Illustration of triggering scheme based on the position of the motorized linear stage. Every time the stage has moved a predefined distance, a Position trigger is sent the ultrasound acquisition system which sets off a series of angled plane-wave transmissions with a set PRF.

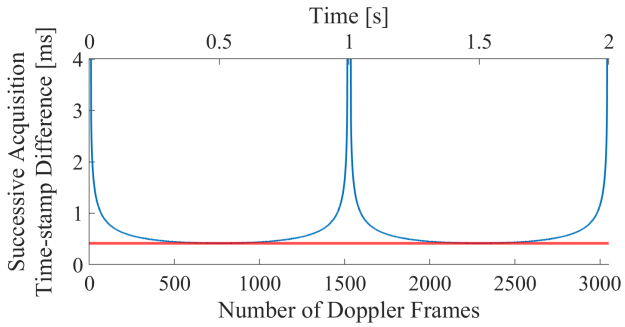

Fig. 4. Time difference between successive samples of a 1-s per sweep trajectory. The red horizontal line depicts the set Doppler FR limit of 2.4 kHz, which the system approaches at the middle of the sweep, where the speed of the motorized stage is highest.

The transmission PRF was set at a fixed 32 kHz. This was taken as high as the system allowed without causing reliability issues and significant temperature changes to the transducer elements. Using a high PRF ensures that the angled plane waves are sampled as close to the position of the input trigger as possible, which is desired when combining them to form a single beamformed image. After transmitting N_a angled plane waves, the system waits for the next trigger to arrive from the motorized stage.

The triggering rate of the motorized stage determines the rate at which Doppler frames (compounded over the N_a angles) will be created. A maximum triggering rate was determined by testing the systems' reliability while using a waveform generator to trigger at increasing frequencies. We found that our system could reliably perform at a Doppler FR of 2.4 kHz. The motorized stage was therefore programmed to never exceed this Doppler FR during its movement trajectory (as the current Doppler FR is determined by the present speed of the motorized stage). This effect is illustrated in Fig. 4, where the difference between successive Doppler frame time stamps is shown over one back-and-forth trajectory. The lowest time between successive Doppler frames, and therefore the highest Doppler frame rate, is reached at the middle of a sweep, where it approaches the set Doppler RF limit (highlighted by the red line).

3) Movement Trajectory: Instead of translating the 1-D-array over the region of interest at a constant speed, the acceleration and deceleration were limited to allow for stable and smooth movement, created by a sinusoidal trajectory. Due to constraints of our motorized stage in combination with the high triggering frame rate, it was not possible to read out the location of each transmission from the motorized stage, requiring us to make a prediction of the location of every frame. During testing, the motor would often overshoot the set location limit, causing an additional frame to be acquired. This resulted in frames no longer being accurately linking to their theoretical locations. This was due to the small scanning region, relatively heavy mass attached to the linear stage, and relatively high movement speeds. The similarity and consistency of successive frames were verified by performing long recordings with many sweeps and looking at the correlation between frames acquired at the same locations. In addition to the sinusoidal trajectory, the servomotor had to be tuned to remove default overshoot correction for proper functionality. These changes as well as changes to the transducer mass made the implemented method stable enough for trajectories with higher speeds.

4) In Vivo Data Acquisition: For in vivo Doppler acquisitions, we used an adult C57Bl/6J mouse ($n = 1$), individually housed under a 12-h light/12-ho dark cycle, with water and food ad libitum. All the experiments were conducted during the light phase and approved by the Institutional Animal Care and Use (IACUC) (Dutch Ethical Committee, Erasmus MC, Rotterdam, The Netherlands) under project license: AVD1010020197846.

a) Surgery: For in vivo Doppler imaging experiments, a pedestal placement was performed to ensure head fixation in the experimental setup. A craniotomy was made to facilitate imaging without attenuating effects of the skull. During surgery, the mouse was anesthetized with an isoflurane/oxygen mixture (5% for induction and 1.75% for maintenance), while the body temperature was kept constant at 37 °C. Also, heart and respiration rate were monitored during surgery (Small Animal Physiological Monitoring System, Harvard Apparatus, MA, USA). This same device was used to fixate and level the skull. Next, a sagittal incision of 2–4 cm in length was made, after which the exposed periosteum was carefully removed. After this, a pedestal (1 × 0.8 cm) was placed on the skull using Optibond (Kerr Bioggio, Switzerland) and a dental cement (Heraeus Kulzer, Armonk, NY, USA) to fixate. The cranial window was performed from Bregma +2 mm to Bregma −4 mm, by 7 mm laterally, and covered by a film of transparent plastic (TPX) (CS Hyde Company, IL, USA). Postoperative mice received 3–5 days of antibiotics (Baytril, 25 mg/ml, Bayer, Germany) to prevent inflammation.

b) Experimental setup: Prior to the start of the imaging experiments, the animal was placed head-fixed on top of a cylindrical foam wheel, where the animal was allowed to walk freely. The animal was habituated five consecutive days for 30 min. During imaging, the ultrasound transducer was placed 4 mm above the cranial window in the coronal plane. Acoustic contact between the transducer and the TPX film was ensured by a small layer of milliQ water topped with a layer of ultrasound transmission gel (Aquasonic 100, Parker Laboratories, NJ, USA).

5) Acquiring Ultrasound Frames: For every swept-3-D sweep, a stack of beamformed images of dimensions (n_z, n_x, n_y) are obtained, where n_z and n_x are the spatial

TABLE I
RELATIONSHIP BETWEEN SINE PERIOD AND NUMBER OF ACQUIRED FRAMES PER VOLUME

Sine Period [s] (2 sweeps)	Maximum Sine Speed [mm/s]	Min Trigger Distance [μm]	Max Frames per Volume
5	3.77	1.57	3819
4	4.71	1.96	3055
3	6.28	2.61	2291
2	9.42	3.93	1527
1	18.85	7.85	763

samples along the z- and x-direction, respectively, and n_y is the number of frames obtained for a sweep. As mentioned in Section II-A2, the frame rate is determined by the displacement of the motorized stage, and therefore, while the distance between frames of n_y is constant during a sweep, the time between successive frames in not. The motorized stage is set to trigger every time the stage has moved by the minimum trigger distance, initiating a burst of eight angled plane waves.

To illustrate the effect of our sinusoidal trajectory on the Doppler FR, and therefore the number of acquired frames, we refer to Table I. First, the maximum velocity is calculated along a sweep for an example craniotomy of 6 mm (details of craniotomy described in more detail in Section II-A4) using $v_{\max} = |\text{Amplitude}|(2\pi/\text{Period})$. The sinusoidal period is variable and determines how long it takes for the motorized stage to complete two sweeps, and it can be altered depending on the use-case (as it has an effect on the Doppler sensitivity). Some example values are shown in Table I, where the case of a sinusoidal period of 5 s implies that two full sweeps are completed within 5 s, granting access to two 3-D PDI volumes. Here, we can see that as the speed of the linear stage is decreased, the amount of frames we can obtain in a sweep is increased. The importance of this relationship will be further investigated on in vivo data in Section II-C.

6) Filtering and Reconstruction: In the conventional stationary power Doppler imaging, a number of beamformed frames are stacked into a space, time matrix of dimensions $(n_z \times n_x, n_e)$, where n_z and n_x are the spatial samples along the z- and x-direction, respectively, and n_e is the number of stacked beamformed frames referred to the ensemble number. This matrix is then filtered by performing a singular value decomposition (SVD) and removing a number of singular components corresponding to stationary and slow moving tissue, leaving the remaining signal to consist of the blood signal and noise [22], [23]. The resulting matrix is averaged over the ensemble length to increase the SNR to create a PDI.

As described in the previous section, our swept-3-D method provides a stack of beamformed frames of dimensions (n_z, n_x, n_y) for every sweep. Unlike in the stationary case, each frame is acquired at a unique location, and therefore, averaging over an ensemble length will impact the resolution in the y-direction. When this matrix is filtered in the same way as the stationary case, where n_y is taken to be the ensemble size n_e, we are left with a stack of low SNR filtered beamformed frames of dimensions (n_z, n_x, n_y). In the swept-3-D case, we are unable to average over n_y, as it contains spatial components from over the whole sweep. Three example frames are shown in Fig. 5, taken from three different locations along a sweep.

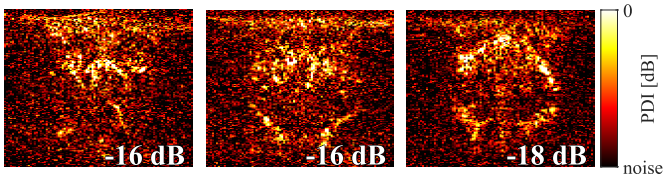

Fig. 5. Collection of three coronal low SNR-filtered beamformed frames before conventional averaging, taken from three different locations along the mouse brain using our swept-3-D method.

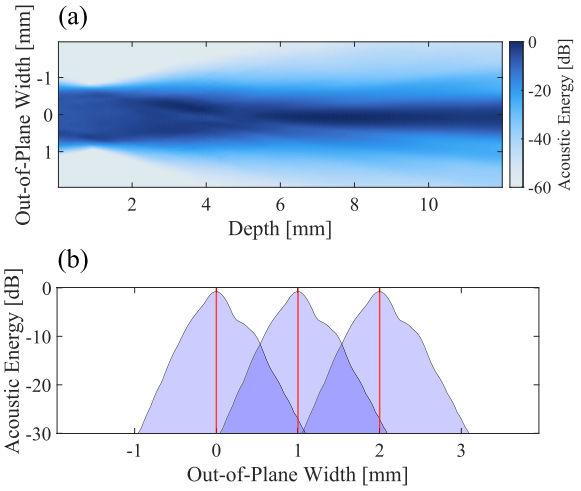

Fig. 6. Combining frames obtained at different y-locations. (a) Out-of-plane (y-axis) beamprofile for our L22-14v ultrasound transducer. (b) Illustration of the overlapping acoustic energy of three frames obtained at locations spaced 1 mm from each other at an imaging depth of 6 mm, with the location highlighted in red.

Even though successive frames are not sampled at the same location, we know that a number of subsequent frames share information due to beam profile of our ultrasound 1-D-array transducer. While we say that our 1-D-array samples a 2-D image of (n_z, n_x), the backscattered energy from a single stationary slice is also influenced by the out-of-plane environment in n_y as can be seen in the out-of-plane beam profile of our ultrasound transducer in Fig. 6(a). The amount of energy in n_y is depth-dependent and also large when compared with the in-plane resolution of the transducer. Fig. 6(a) is obtained using a hydrophone scan plane at a depth of 4 mm and subsequent angular spectrum propagation to estimate the beamprofile at every depth [24]. No attenuation in the spectral propagator or hydrophone directivity compensation was applied. Fig. 6(b) shows an illustration of how much energy is shared by three frames obtained at 1-mm intervals. In practice, when we look at Table I, a travel distance of 1 mm in n_y can contain more than 600 frames when using a sine period of 5 s.

Instead of filtering a whole sweep, the images can be split into a number of repeated ensembles of dimensions $(n_z \times n_x, n_e, n_{\text{rep}})$ which gives us a situation similar to that of the stationary method, meaning it can be SVD-filtered in a similar fashion over every ensemble n_e. After averaging over

n_e, it would leave us with a number of PDIs spanning across the mouse brain, in a similar way to the stationary case.

As we are continuously moving during the acquisition of an ensemble of data with our swept-3-D method, the location at which each beamformed frame is acquired is unique. To reconstruct a PDI for a specific location y_i, we want to include the spatially closest frames from each side in the ensemble from $(y_i - n_e/2, y_i + n_e/2)$. However, we do not know whether all the frames should be weighted equally in the averaging, as frames acquired further from y_i contain less shared information than those acquired close to it. Choosing the ensemble number has a lot more consequences when compared with stationary recordings, as you need a number of frames high enough for good delineation of tissue and blood motion without losing the spatial coherence of the frames within an ensemble. This effect will be investigated further for in vivo data in Section II-C.

For the visualization of each PDI in this article, the image is normalized to the highest 99.5% value of the image. The average noise level is calculated by averaging the image values in the first five rows, in which there is no vasculature present. (Note: These are all the lateral samples of the displayed/cropped image, not of the samples acquired directly under the transducer.) Values lower than the average noise level are set to the average noise level. When multiple PDIs are displayed in the figures, the average noise level is overlaid in the corner of the image.

B. Doppler Spectrum

The functionality of our proposed imaging method was verified using custom 3-D-printed flow phantoms. The phantoms were 3-D-printed using a 3-D resin material (HTM140, EnvisionTEC, Gladbeck, Germany) and consist of two slanted hollow tubes that allow for flow. The tubes have an outer diameter of 1.2 mm and an inner diameter of 1 mm, which was the thinnest wall thickness that could reliably be printed for our inner diameter using our 3-D resin printer. The bottom two nozzles were connected by tubing to a syringe filled with blood-mimicking Doppler fluid (CIRS, Model 769DF) and placed in a syringe pump (PHD ULTRA, Harvard Apparatus, MA, USA). The top two nozzles were connected by tubing to a fluid reservoir to allow for a looped flow system. The phantom contains a rectangular window of 12 × 12 mm with a depth of 15 mm, which can be filled with water or a tissue mimicking substance. The dimensions were chosen to be close to the ones used in the mouse brain, allowing for an accurate representation of travel distances and depth measurements. The ultrasound transducer was placed on top of the phantom, using a layer of water to make contact for acoustic coupling.

To validate the obtained swept-3-D data, it was compared with data obtained during a stationary recording by analyzing the Doppler spectrum. During the first experiment, the transducer was placed roughly over the center of the flow phantom's tube, and short acquisitions were recorded for varying flow rates. As the reconstructed PDIs for the varying flow rates are very similar, a single PDI for the lowest flow rate is shown in Fig. 7(a). Fig. 7(b)–(d) shows spectrograms for three increasing flows of 0.3, 0.4, and 0.5 ml/min, respectively.

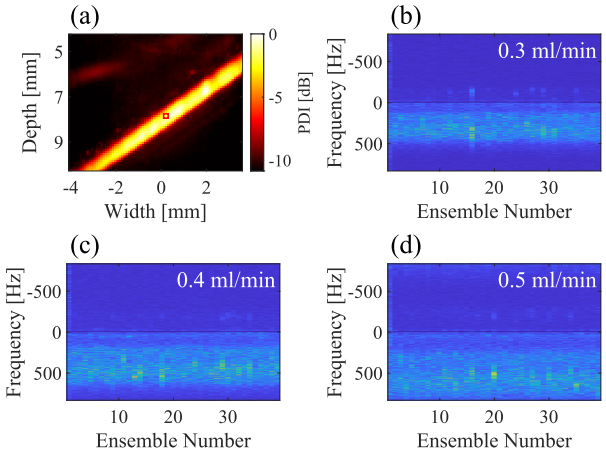

Fig. 7. Doppler spectrum in flow phantom. (a) PDI reconstructed for a stationary recording using a flow rate of 0.3 ml/min. (b)–(d) Three spectrograms reconstructed for flow rates of 0.3, 0.4, and 0.5 ml/min, respectively.

The goal of the next experiment was to see how accurately the PDI obtained from a swept recording could be reconstructed while continuously moving over the flow phantom, as well as to investigate the effect of varying Doppler flow rates, and varying transducer movement speeds on the obtained spectrum. First, the flow rate was kept constant at 0.4 ml/min while the transducer was swept over the ultrasound flow phantom in 2.5, 5, and 10 s, respectively, as seen in the top half of Fig. 8. Due to the varying speeds of the motorized stage and the fixed frame rate, a different number of Doppler frames were acquired for each of the sweeps. This becomes evident when looking at the reconstructed spectrograms shown in Fig. 8(d)–(f). Here, a spectrogram is created by taking an ensemble of 100 Doppler frames, filtering it using an SVD and removing the components corresponding to stationary/and slow moving material, and then repeating this process for the next 100 Doppler frames till the end of the sweep is reached. As the motorized stage has a higher speed for the spectrogram on the left, less ensembles of 100 frames are created for the sweep. When looking at the reconstructed PDIs for each of the swept sweeps, shown in Fig. 8(a)–(c), the reconstructed PDI using the highest speed has a less good removal of the stationary tissue components due to the larger distance between successive frames. The average frequency spectrum over ten ensembles is shown in Fig. 9(a), showing a higher center frequency for an increased flow rate, as well as increased spectral broadening. Fig. 9(b) shows the frequency spectrum reconstructed for the ensemble obtained closest to the location of the stationary recording from Fig. 7, indicated by a vertical red line in Fig. 8(d)–(f), where we can see that all the three recordings contain similar frequency information.

A second experiment was done to mimic the varying flow rates used in the stationary experiment (Fig. 7 with 0.3, 0.4, and 0.5 ml/min, respectively) while maintaining a constant sweep time of 10 s per sweep. The same method is used for creating the spectrograms, PDIs, and frequency spectra as in the previous experiment. As with the previous experiment, the frequency spectrum for each of the varying flow rates is shown

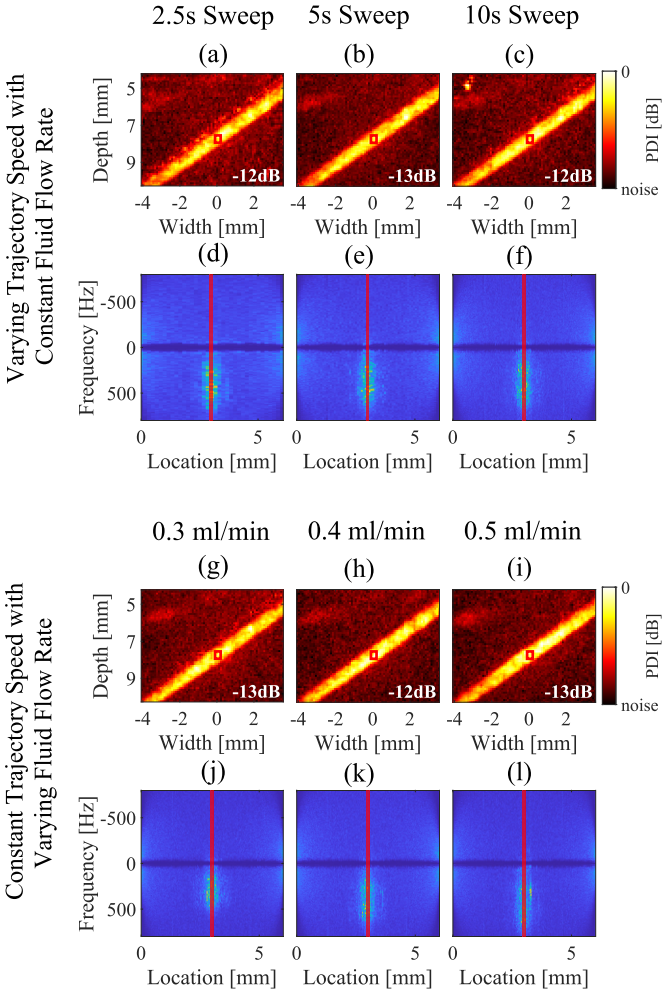

Fig. 8. Swept-3-D Doppler spectrum reconstructed for every 100 frames over a sweep, with a PDI reconstructed at the location closest to the stationary recording of Fig. 7 using a varying trajectory speed with constant Doppler flow rate (a)–(f) and constant trajectory speed (10 s per sweep) with varying Doppler flow rate (g)–(l).

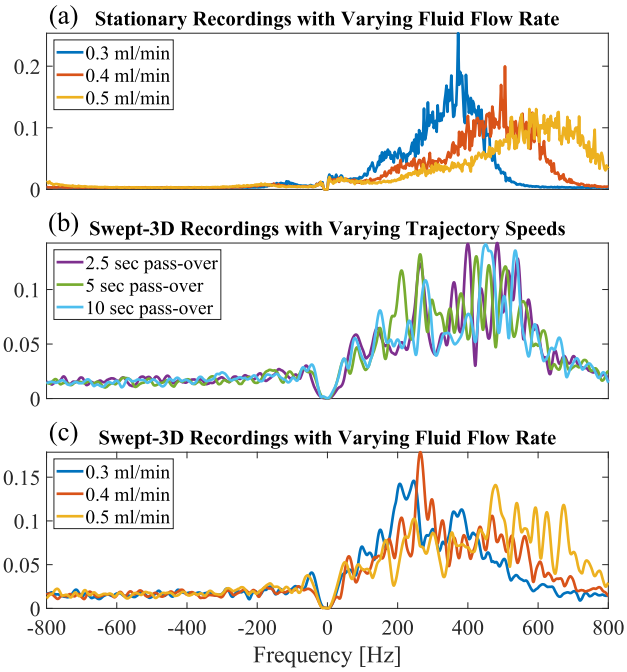

Fig. 9. Doppler spectrum of flow phantom. (a) Doppler spectrum obtained from a stationary recording for three different Doppler flow rates of 0.3, 0.4, and 0.5 ml/min. (b) Swept-3-D Doppler spectrum obtained from three sweep speeds for a constant Doppler flow rate of 0.4 ml/min. (c) Swept-3-D Doppler spectrum obtained for the same Doppler flow rates as used in (a).

in Fig. 9(c), where the same pattern of increasing Doppler center frequency with increasing flow speed can be found as shown in the stationary recording from Fig. 7. We can see that the noise level and Doppler peak bandwidth for the swept 3-D case are significantly higher than in the stationary case.

C. In Vivo Doppler Reconstruction

The goal of this work was to create 3-D Doppler reconstructions that most closely resemble those obtained during a stationary recording, and therefore, this section will look at how to best combine the low SNR-filtered beamformed frames obtained in Section II-A6 of dimension (n_z, n_x, n_y).

In Fig. 10, a moving average filter of different lengths was applied over the y-direction of the filtered data, where every frame was weighted equally. The moving average filters of lengths 400, 200, 100, 50, and 1 frame(s) were taken to resemble averaging over an ensemble of the respective lengths. The top two rows of Fig. 10 show the resulting in-plane Doppler image for two different locations along a sweep, and out-of-plane images are shown on the bottom row. When looking at the left column, for a filter length of 400 frames, while the in-plane SNR appears to be high, the out-of-plane signal has lost a lot of the detail when compared with filtering with a lower number of frames. Many of the high-intensity vessels appear over a larger area in the y-axis due to excessive averaging. Therefore, the ideal combination of frames most likely lies somewhere in between these extremes. The second half of Fig. 10 shows the same processing steps on a recording with a sine period of 2 s (1 s sweep time), where the filter is unable to remove the majority of the motion artifacts, as well as having more smearing in the out-of-plane direction due to the larger distance between successive frames.

With the high-precision motorized linear stage, it was possible to perform both staged recordings and swept-3-D recordings in quick succession without altering the physical setup. Staged recordings were performed on head-fixed mice as described in Section II-A4 by recording 5 s of high frame rate ultrasound data for every slice and filtering it using the methods described in Section II-A6 to create a single PDI. This process was repeated every 100 μm, usually resulting in about 70 PDIs with a craniotomy of 7 mm. As the physical location of the mouse remained the same during recordings of the two methods, locations of each slice of the brain could be directly compared.

To better understand our swept-3-D data, data were acquired using multiple sine periods and reshaped into beamformed frames of dimension (n_z, n_x, n_y). For the left column of Fig. 11, the full sweep was decomposed using an SVD, and a varying percentage of n_y components were removed as shown in the y-axis. A PDI was reconstructed by averaging

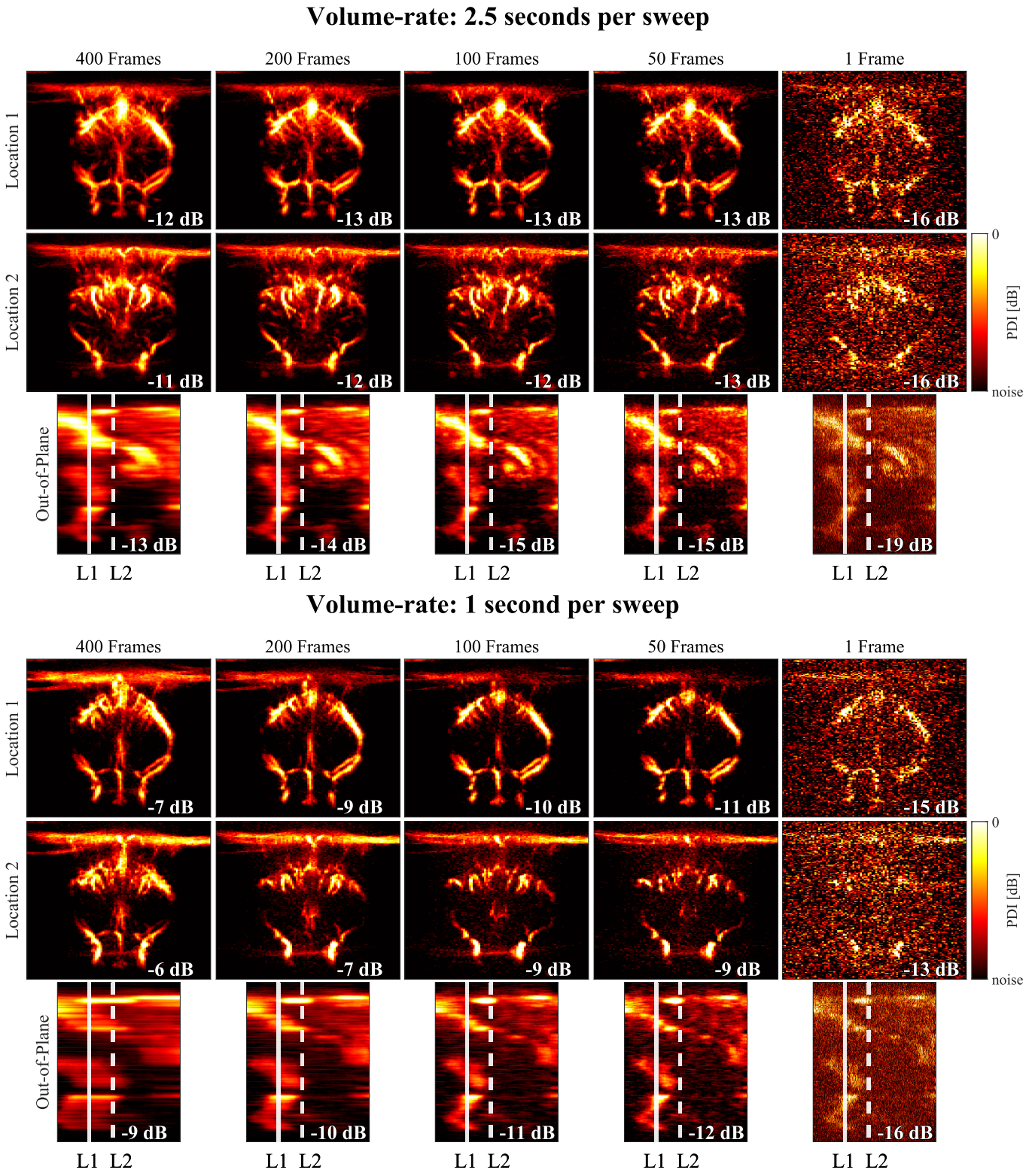

Fig. 10. Averaging of coronal swept-3-D frames over a sweep for two different trajectory speeds. The top three rows contain swept-3-D data from a 2.5 s sweep time, where for each column a PDI was created by averaging over the specified number of frames. This is shown for two locations, as indicated in the out-of-plane images in the third row. This process was repeated for a swept-3-D recording with a sweep time of 1 s in the following three rows.

over a varying number of frames surrounding the location of the stationary reference frame in the x-axis. For each PDI created, the MSE was calculated between the reference PDI and the swept-3-D PDI for the sine periods of 5, 4, 3, and 2. For illustrative purposes, a PDI is reconstructed for a point for each of the different sweeping speeds (200 averaged frames, 14 removed components), as highlighted by a red diamond shape in each of the figures, to show the effect of translation

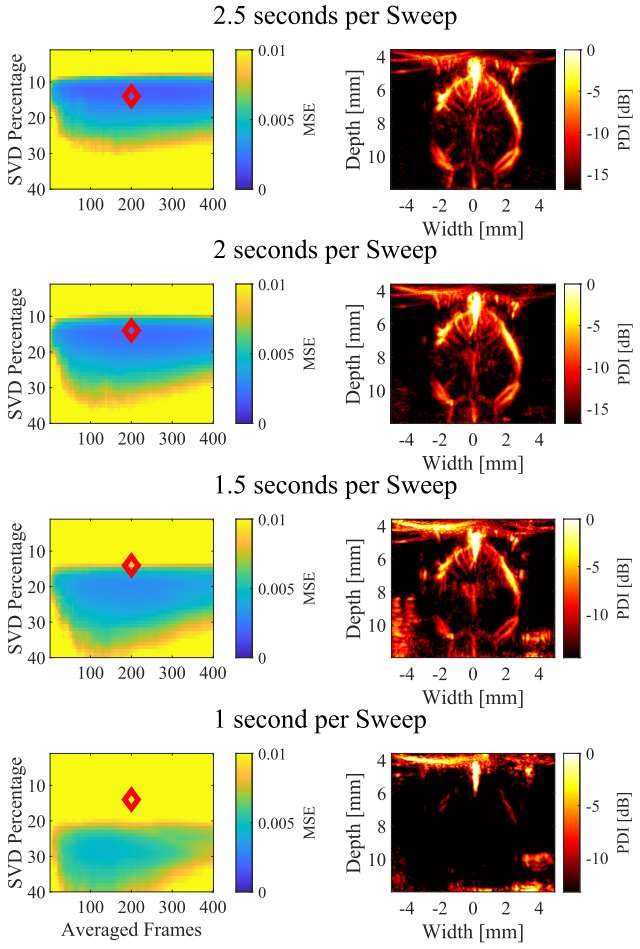

Fig. 11. Comparison of sweeping speeds. For each different sweeping sweep, the MSE is calculated between a PDI from a stationary recording and those created using swept-3-D frames for varying SVD clutter filter percentages and number of frames averaged (left). For illustrative purposes, a PDI is reconstructed for 200 averaged frames, and 14 removed components (red diamond) for each of the sweep times (right).

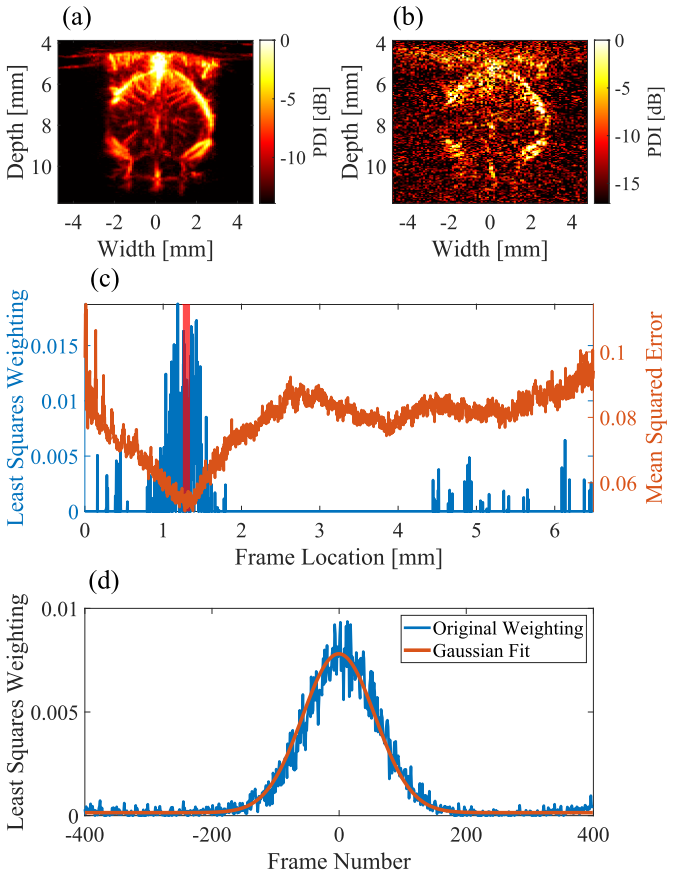

Fig. 12. Comparing a stationary PDI to swept-3-D frames. (a) PDI reconstructed for a stationary recording. (b) Single swept-3-D beamformed frame from the same location as the stationary recording. (c) MSE and least-squares weighting obtained for each frame of a swept-3-D sweep with the location of the reference frame shown by the red vertical line. (d) Least-squares weighting obtained after averaging weightings obtained for every stationary recording.

speed on the resulting PDIs, and is shown in the right column. Here, we can see that the MSE is larger for increasing trajectory speeds, with more clutter signal remaining in the higher speed recordings.

Instead of averaging over an arbitrary number of frames, we decided to search for a method for finding a weighting window to create the best vascular images.

To find what linear combination of low SNR swept-3-D frames can be used to best recreate a PDI obtained from a stationary recording, the following least-squares cost function can be solved:

$$\min_{w} \|Cw - d\|_2^2, \quad \text{where } w \geq 0 \tag{1}$$

where d is the high-quality staged PDI that can be used as a reference of dimension $(n_z \times n_x, 1)$, C is the system matrix containing all the low SNR-filtered beamformed frames from a sweep with dimensions $(n_z \times n_x, n_y)$ as previously described in Section II-A6, and w is the weighting vector of interest with dimensions $(n_y, 1)$. The constraint on w was chosen to not allow negative contributions of frames.

A PDI is shown in Fig. 12(a) obtained from a stationary recording using an ensemble length of 200 beamformed frames. A single swept-3-D beamformed frame is shown in Fig. 12(b), which was obtained at the same location as the previous stationary recording. The MSE and weighting vector w for a single frame are shown in Fig. 12(c). The reference PDI was acquired close to the caudal end of the craniotomy, roughly 1.5 mm from the starting location of the trajectory (depicted by the red vertical line in the plot on the right). The weighting vector w mainly contains contributions from frames within 0.5 mm of the staged reference frame.

This process was repeated for all the staged reference frames. Instead of using the full sweep, a window of 800 frames was taken around each reference frame so they could be compared with each other. The averaged weightings are shown in Fig. 12(d). As the final weighting remains noisy and the shape resembles that of a normal distribution, a Gaussian fit was applied so this weighting vector could be used to create the final 3-D PDIs.

Fig. 13 shows the swept-3-D PDIs for a single sweep. Here, a PDI is reconstructed by applying the weighting to a filtered ensemble of swept-3-D data with steps of 200 μm between every reconstruction. The approximate location of

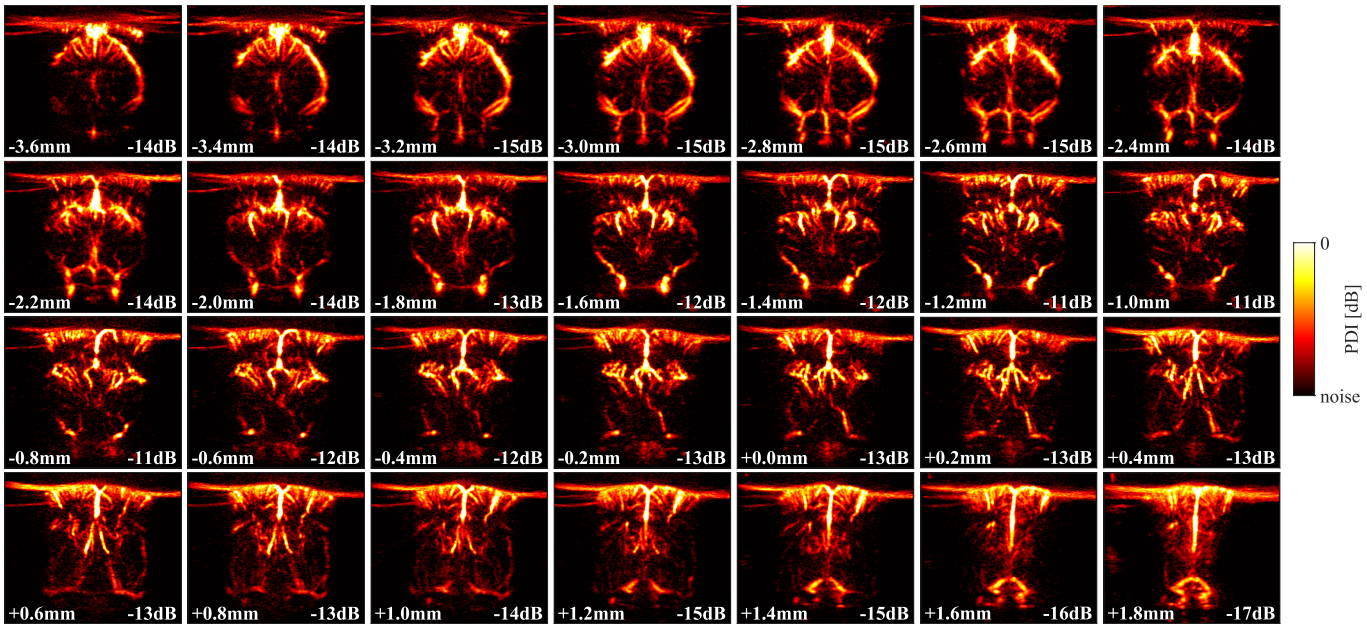

Fig. 13. Swept-3-D power Doppler imaging. A PDI is reconstructed every 200 μm starting from the caudal section (top left) to the most rostral (bottom right). The locations listed in the bottom right of every PDI show its approximate distance relative to Bregma.

every reconstructed PDI is shown in the bottom right relative to Bregma. The artifacts on the cortex of the most rostral and caudal images, and on the most lateral sections of most PDIs, are caused by backscattered energy from intact sections of skull that is unable to be properly filtered.

III. Discussion and Conclusion

In this article, we tried to find a method to most accurately reconstruct a PD volume while continuously moving an ultrasound transducer over the mouse brain. We did this by comparing the swept-3-D ultrasound data to that acquired in conventional stationary recordings. For this, we used a very high-precision motorized linear stage, which remained accurate under the relatively large load of the transducer. By removing the casing, and creating sturdy yet lightweight custom mount (Fig. 2), the ultrasound 1-D-array could be reliably and precisely moved back-and-forth over the mouse brain. Due to the limitations in the maximum triggering frequency of the linear stage, the ultrasound system was programmed to transmit eight angled plane waves for every received trigger from the stage. If the hardware would have allowed for it, it might have been beneficial to trigger for every angle so that the exact location and timing of every transmission were known. The effect of this limitation was minimized by unlinking the PRF between sets of angled transmissions. Within a single set of angles, the PRF was set to 32 kHz, while after a set of eight angles had been transmitted the system waited for an external position trigger (Fig. 3). This ensured that the set of angles corresponding to a trigger was as close to the initial location as possible. Another constraint was caused by the acquisition system itself, when using a too high PRF the data could no longer be processed in real-time, causing the system to miss triggers, leaving gaps in the data. This was particularly tricky as the location of every frame is estimated in postprocessing based on its expected location. Since the Doppler reconstruction stages are performed in postprocessing for the swept-3-D method, the computational load could have been lowered by no longer applying real-time filtering to the acquired data, or by directly storing the raw RF data.

The data presented in this article were obtained on awake head-fixed adult mice, by imaging through a cranial window covered by a TPX layer, while the mice were able to freely walk on a rotating wheel. A cranial window is not always necessary if the mouse is at a young age, though the signal attenuation starts to increase drastically as the age of the mouse increases, and therefore, it was decided to use a cranial window in this article. The mice were habituated in the setup until they were found to no longer present signs of stress, to minimize unwanted movement during recordings. Alternatively, motion artifacts can be reduced using anesthetized mice instead of awake/head-fixed mice; however, this can be less desirable for functional recordings.

Frames obtained using our swept-3-D method are all acquired at unique locations; however, information between successive frames is shared due to the out-of-plane resolution of the transducer (Fig. 6). This is particularly true for high-frequency 1-D-arrays which are required when imaging the mouse brain, where the out-of-plane resolution is much lower than the in-plane resolution, meaning that there is more spatial coherence between successive frames. In situations where the scanning region is much larger and a lower frequency 1-D-array is desired, such as when imaging the human brain, the viability has to be investigated. Lower frequency arrays generally make use of larger transducer elements, which in turn increases the mass of the resulting transducer. This effect together with the potentially higher speed of the motorized stage due to the large scanning surface can heavily affect the resulting PDIs. The sinusoidal trajectory of the motorized stage used in the article may not be necessary when scanning larger regions as the deceleration of the stage can take place over a longer time, allowing the stage to move at the maximum velocity for a longer period during the sweep. Moving toward

a compact enclosure for the motorized stage and ultrasound transducer, as is the case with the Wobbler, would help provide a safe packaged system suitable for free-hand scanning which would allow for a larger variety of imaging applications such as in a clinical setting, for example, during awake brain tumor removal surgery, where the surgeon has direct access to the patients brain and 3-D brain Doppler volumes could be provided. The viability needs to be further investigated due to the cumbersomeness of the high-precision motorized stage's added weight, which may restrict handheld scanning.

PDIs obtained during stationary recordings were compared with frames obtained with our swept-3-D method. There are many methods to compare a set of images, such as computing the MSE, correlation, or structural similarity index [25] to name a few. The results obtained from each of these tested algorithms did not always fall in line with a human's interpretation, allowing room for future improvements. Due to the unique nature of our swept-3-D acquisitions, it would make sense to investigate alternative filtering methods to separate the blood subspace from the tissue subspace. Subspace tracking methods [26] have been shown on fUS [27], where the algorithm is able to filter a single beamformed frame at a time, instead of being restricted by the typical ensemble of frames.

The presented spatial sampling in the out-of-plane direction was constant throughout a sweep, meaning that the PRF varies for different spatial regions along the trajectory. Alternatively, the PRF can be kept constant causing the spatial sampling to vary. The effects of both the methods on the optimal filtering for each location need to be investigated in future research.

The final swept-3-D PDIs were reconstructed over a whole sweep every 200 μm (Fig. 13). The distance between every PDI reconstruction was taken as 200 μm for visualization purposes, as due to the continuous nature of our swept-3-D acquisitions, we are not restricted to the step size determined by the conventional acquisition locations of a staged recording.

In conclusion, in this article we presented a method for volumetric 3-D Doppler imaging using a continuously moving linear stage. We are able to maintain good sensitivity, low computational complexity, and monetary cost when compared with the use of 2-D matrix probes, while not requiring repeated recordings for every slice as when using a 1-D-array transducer in a staged fashion. The resulting PDIs from our swept-3-D method provide detailed vasculature similar to PDIs obtained during a 1-D-array stationary recording, allowing for more efficient atlas registration in the neuroscientific context, and path the way for fUS imaging which is the topic of the second part of this article.

Acknowledgment

Bastian S. Generowicz, Stephanie Dijkhuizen, and Sebastiaan K. E. Koekkoek are with the Department of Neuroscience, Erasmus MC, 3000 CA Rotterdam, The Netherlands.

Chris I. De Zeeuw is with the Department of Neuroscience, Erasmus MC, 3000 CA Rotterdam, The Netherlands, and also with the Royal Dutch Academy of Arts and Sciences, Netherlands Institute for Neuroscience, 1105 BA Amsterdam, The Netherlands.

Pieter Kruizinga is with the Department of Neuroscience, Erasmus MC, 3000 CA Rotterdam, The Netherlands, and also with the Faculty EEMCS, Delft University of Technology, 2628 CD Delft, The Netherlands (e-mail: p.kruizinga@erasmusmc.nl).

References

[1] G. Montaldo, M. Tanter, J. Bercoff, N. Benech, and M. Fink, "Coherent plane-wave compounding for very high frame rate ultrasonography and transient elastography," *IEEE Trans. Ultrason., Ferroelectr., Freq. Control*, vol. 56, no. 3, pp. 489–506, Mar. 2009.

[2] M. Tanter and M. Fink, "Ultrafast imaging in biomedical ultrasound," *IEEE Trans. Ultrason., Ferroelectr., Freq. Control*, vol. 61, no. 1, pp. 102–119, Jan. 2014.

[3] E. Macé, G. Montaldo, I. Cohen, M. Baulac, M. Fink, and M. Tanter, "Functional ultrasound imaging of the brain," *Nature Methods*, vol. 8, pp. 662–664, May 2011.

[4] J. Provost et al., "3D ultrafast ultrasound imaging in vivo," *Phys. Med. Biol.*, vol. 59, no. 19, p. L1, 2014.

[5] C. Rabut et al., "4D functional ultrasound imaging of whole-brain activity in rodents," *Nature Methods*, vol. 16, no. 10, pp. 994–997, Oct. 2019.

[6] J. Sauvage et al., "4D functional imaging of the rat brain using a large aperture row-column array," *IEEE Trans. Med. Imag.*, vol. 39, no. 6, pp. 1884–1893, Jun. 2020.

[7] C. E. Morton and G. R. Lockwood, "Theoretical assessment of a crossed electrode 2-D array for 3-D imaging," in *Proc. IEEE Symp. Ultrason.*, Mar. 2003, pp. 968–971.

[8] G. R. Lockwood, J. R. Talman, and S. S. Brunke, "Real-time 3-D ultrasound imaging using sparse synthetic aperture beamforming," *IEEE Trans. Ultrason., Ferroelectr., Freq. Control*, vol. 45, no. 4, pp. 980–988, Jul. 1998.

[9] S. Blaak et al., "Design of a micro-beamformer for a 2D piezoelectric ultrasound transducer," in *Proc. IEEE Int. Ultrason. Symp.*, Sep. 2009, pp. 1338–1341.

[10] D. B. Downey and A. Fenster, "Vascular imaging with a three-dimensional power Doppler system," *Amer. J. Roentgenol.*, vol. 165, no. 3, pp. 665–668, 1995.

[11] C. Demené et al., "4D microvascular imaging based on ultrafast Doppler tomography," *NeuroImage*, vol. 127, pp. 472–483, Feb. 2016.

[12] M. Gesnik et al., "3D functional ultrasound imaging of the cerebral visual system in rodents," *NeuroImage*, vol. 149, pp. 267–274, Apr. 2017.

[13] R. Rau et al., "3D functional ultrasound imaging of pigeons," *NeuroImage*, vol. 183, pp. 469–477, Dec. 2018.

[14] S. Meairs, J. Beyer, and M. Hennerici, "Reconstruction and visualization of irregularly sampled three- and four-dimensional ultrasound data for cerebrovascular applications," *Ultrasound Med. Biol.*, vol. 26, no. 2, pp. 263–272, Feb. 2000.

[15] S. Soloukey et al., "Functional ultrasound (fUS) during awake brain surgery: The clinical potential of intra-operative functional and vascular brain mapping," *Frontiers Neurosci.*, vol. 13, p. 1384, Jan. 2020.

[16] C. Chen et al., "In vivo 3D power Doppler imaging using continuous translation and ultrafast ultrasound," *IEEE Trans. Biomed. Eng.*, vol. 69, no. 3, pp. 1042–1051, Mar. 2022.

[17] R. W. Prager, U. Z. Ijaz, A. Gee, and G. M. Treece, "Three-dimensional ultrasound imaging," *Proc. Inst. Mech. Eng., H, J. Eng. Med.*, vol. 224, no. 2, pp. 193–223, 2010.

[18] Z. Dong et al., "High volume rate 3-D ultrasound imaging using fast-tilting and redirecting reflectors," *IEEE Trans. Ultrason., Ferroelectr., Freq. Control*, vol. 70, no. 8, pp. 799–809, Aug. 2023.

[19] S. M. Sunkin et al., "Allen brain atlas: An integrated spatio-temporal portal for exploring the central nervous system," *Nucleic Acids Res.*, vol. 41, no. D1, pp. D996–D1008, Nov. 2012.

[20] G. Paxinos and C. Watson, *The Rat Brain in Stereotaxic Coordinates: Hard Cover Edition*. Amsterdam, The Netherlands: Elsevier, 2006.

[21] J. Bercoff et al., "Ultrafast compound Doppler imaging: Providing full blood flow characterization," *IEEE Trans. Ultrason., Ferroelectr., Freq. Control*, vol. 58, no. 1, pp. 134–147, Jan. 2011.

[22] L. A. F. Ledoux, P. J. Brands, and A. P. G. Hoeks, "Reduction of the clutter component in Doppler ultrasound signals based on singular value decomposition: A simulation study," *Ultrason. Imag.*, vol. 19, no. 1, pp. 1–18, Jan. 1997.

[23] C. Demené et al., "Spatiotemporal clutter filtering of ultrafast ultrasound data highly increases Doppler and fUltrasound sensitivity," *IEEE Trans. Med. Imag.*, vol. 34, no. 11, pp. 2271–2285, Nov. 2015.

[24] P. Kruizinga et al., "Compressive 3D ultrasound imaging using a single sensor," *Sci. Adv.*, vol. 3, no. 12, Dec. 2017, Art. no. e1701423.

[25] Z. Wang, A. C. Bovik, H. R. Sheikh, and E. P. Simoncelli, "Image quality assessment: From error visibility to structural similarity," *IEEE Trans. Image Process.*, vol. 13, no. 4, pp. 600–612, Apr. 2004.

[26] B. Yang, "An extension of the PASTd algorithm to both rank and subspace tracking," *IEEE Signal Process. Lett.*, vol. 2, no. 9, pp. 179–182, Sep. 1995.

[27] B. Generowicz et al., "Efficient and flexible spatiotemporal clutter filtering of high frame rate images using subspace tracking," in *Proc. IEEE Int. Ultrason. Symp. (IUS)*, May 2018, pp. 206–212.

Bastian S. Generowicz was born in The Netherlands, in 1990. He received the B.Sc. degree in electrical engineering and the M.Sc. degree (electrical engineering) in the signals and systems track from the Delft University of Technology, Delft, The Netherlands, in 2016 and 2019, respectively. He is currently pursuing the Ph.D. degree with the Department of Neuroscience, Erasmus MC, Rotterdam, The Netherlands.

His field of research focused on applying advanced signal processing techniques to the field of Doppler ultrasound imaging. At present he is developing new techniques for 3-D functional ultrasound and 3-D Doppler imaging of the brain.

Stephanie Dijkhuizen was born in Delft, The Netherlands, in 1991. She received the B.Sc. degree in biomedical science from Hogeschool Leiden, Leiden, The Netherlands, in 2016.

In 2017, she joined the Associative Learning Laboratory, Erasmus MC, Rotterdam, The Netherlands. In 2019, she joined the Center for Ultrasound Brain Imaging Erasmus MC (CUBE), Department of Neuroscience, Erasmus MC. Her current field of research focuses mainly on associative learning using Pavlovian eyeblink conditioning.

Chris I. De Zeeuw was born in Gouda, The Netherlands, in 1960. He received the M.D. and Ph.D. degrees (cum laude) from Erasmus MC, Rotterdam, The Netherlands, in 1990 and 1991, respectively.

He was a Co-Founder of CUBE. Since 1998, he has been the Chair of the Department of Neuroscience, Erasmus MC, as well as a Scientific Vice-Director of the Netherlands Institute for Neuroscience, Royal Dutch Academy of Arts and Sciences (KNAW), Amsterdam, The Netherlands. His research has led to unprecedented insights on how the brain, in particular the cerebellum, may control simple forms of learning like adaptation and conditioning of eye movements and eyeblinks.

Sebastiaan (Bas) K. E. Koekkoek was born in Eindhoven, The Netherlands, in 1970. He received the B.Sc. and master's degrees in medicine from Erasmus MC, Rotterdam, The Netherlands, in 1996, and the Ph.D. degree from the Department of Neuroscience, Erasmus MC, in 2004.

He was a Postdoctoral Researcher and holds a permanent position as an Assistant Professor. He is the PI of the Associative Learning Laboratory, Department of Neuroscience and a Co-Founder of Center for Ultrasound Brain Imaging Erasmus MC (CUBE), Erasmus MC. Next to his pure scientific work, he has been active as a General Manager of Neurasmus B.V., Rotterdam, where he was an in charge of development and valorization of new scientific tools. More recently, he operates as a Co-Founder and CSO of BlinkLab Pty, Sydney, Australia, where he oversees scientific work, creates data analysis tools, and safeguards data quality. BlinkLab develops a smartphone-based platform for neuroscience and diagnosis of neurodevelopmental and psychiatric disorders.

Pieter Kruizinga received the Ph.D. degree from Erasmus MC, Rotterdam, The Netherlands, in 2015.

In 2018, he joined the Neuroscience Department, Erasmus MC, where he leads the imaging research within the Center for Ultrasound and Brain-Imaging Erasmus MC (CUBE). His current research focuses on computational ultrasound imaging and functional ultrasound imaging of the brain.